

RADAR OBSERVATIONS OF LUNAR HOLLOW TERRAIN. Lynn M. Carter¹, B. Ray Hawke², W. B. Garry¹, Bruce A. Campbell³, T. A. Giguere², and D. B. J. Bussey⁴, ¹NASA Goddard Space Flight Center, Planetary Geodynamics Lab Code 698, Greenbelt, MD 20771, lynn.m.carter@nasa.gov, ²Hawaii Institute of Geophysics and Planetology, University of Hawaii, Honolulu HI 96822, ³Center for Earth and Planetary Studies, Smithsonian Institution, Washington DC 20013, ⁴The Johns Hopkins University Applied Physics Lab, Laurel, MD, 20723.

Introduction: Distinctive lunar hollows with disrupted rough surfaces have been recognized since the 1970s (e.g. [1]). The Ina caldera-like feature is a well known, large (3 km), and particularly clear example of these unusual terrains [2]. These features have characteristic morphologic features that include a rough, lower-elevation surface with irregularly shaped boundaries, steep edges, and smooth-surfaced mounds. On the Moon, hollows are often found in volcanic settings [3, 4]. Numerous formation mechanisms have been proposed, including recent outgassing [3] and lava flow inflation [5].

Disrupted terrains similar to lunar hollows have also been identified on Mercury and Mars. On Mercury, the hollows have primarily been found associated with

the interior floors of impact craters, suggesting that their formation requires the release of deep-interior volatiles [6]. The Mercury hollows are interpreted as collapse features formed by the release of volatiles through outgassing, sublimation, space weathering, or pyroclastic volcanism [6]. On Mars, flow inflation has created terrain with similar morphologic features to the lunar hollows [7].

Radar observations of lunar volcanic features have shown that some surfaces, including some of the hollows, are surrounded by fine-grained, block-free material that is consistent with pyroclastics. However, the hollow terrains exhibit a variety of different radar backscatter properties. In particular, the circular polarization ratio (CPR) associated with the hollows varies

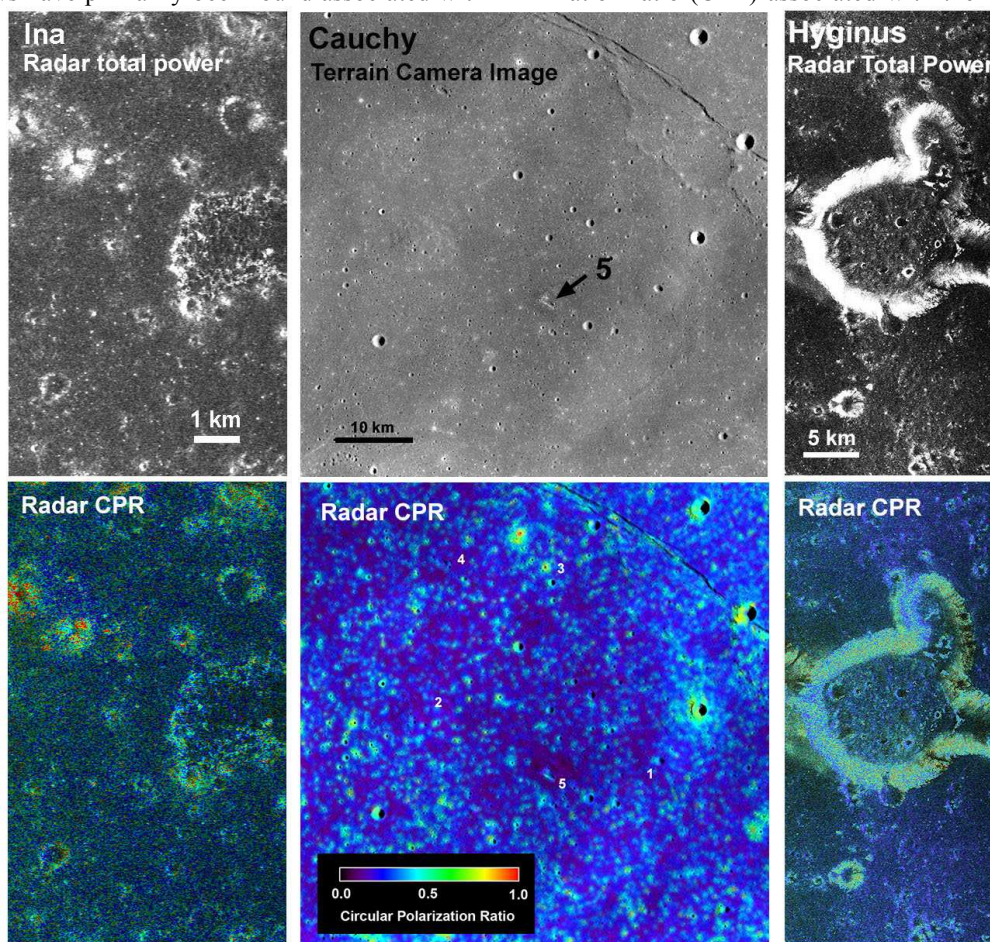


Fig. 1: Radar CPR data of lunar hollows; all data use the same color scale. *Ina*: Top is a Mini-RF total power radar image, bottom is CPR overlaid on radar total power. *Cauchy region*: Top is Kaguya Terrain Camera image, bottom is ground-based radar CPR overlaid on the Kaguya image. Cauchy 5 is marked. *Hyginus*: Top is a Mini-RF total power radar image, bottom is CPR overlaid on radar total power.

significantly, implying a different near-surface structure at the different sites.

Ina: Ina (18.7° N, 5.3° E) consists of a D-shaped depression, 3 km wide and 64 m deep, that sits at the top of a low dome. Radar data (S-band, 12.6 cm wavelength, 15x30 m resolution) from the Mini-RF instrument on the Lunar Reconnaissance Orbiter spacecraft [8] show enhanced CPR (Fig. 1) from the edges of the Ina depression and from the interior blocky terrain mapped by [5]. There is virtually no change in the CPR across smooth portions of the ~15 km dome. CPR values across the dome are similar to those of the surrounding cratered plains, suggesting that there is not a significant change in the near-surface bulk properties (e.g. rock abundance) at Ina.

Cauchy 5: A survey of several lunar dome fields using S-band (12.6 cm wavelength, 80 m resolution) ground-based radar data taken with the Arecibo and Green Bank Telescopes [9] revealed that the Cauchy 5 dome (7.2° N, 37.6° E) has a CPR value of 0.1, which is among the lowest values measured for any lunar dome (Fig. 1). Mini-RF has not collected data for this dome. Subsequent imaging by the LROC NAC has revealed that the caldera of this ~5 km diameter dome is similar in many ways to Ina (Fig. 2). The long linear caldera-like feature is surrounded by irregular pits that extend ~1 km from the dome center. Some of the pits are fairly circular but have ragged or incomplete edges that suggest that they are either not impact related, or were modified after formation. A low-albedo region surrounds the caldera and appears to match the extent of the low-CPR area in the radar data. The low CPR indicates that the upper centimeters to meter of this dome is composed of fine-grained, block poor material, potentially a fairly pure pyroclastic deposit.

Hyginus: The floor of the volcanic Hyginus crater (7.8° N, 6.3° E; 11 km diameter) has high-albedo regions within depressions that have been interpreted as collapse features caused by volatile release [1]. The crater floor is often listed as an additional example of hollow terrain [2,4]. Low optical albedo terrain surrounding the crater suggests pyroclastics [10], and ground-based radar CPR values are similar to those measured at the nearby Vaporum pyroclastic [11]. Mini-RF CPR measurements within the caldera have slightly higher CPR values than the surrounding pyroclastics (Fig. 1). This can also be seen in the prior ground-based data [11], and may be due to the presence of rough hills and knobs inside the caldera. Alternatively, the pyroclastics may have been distributed primarily outside the caldera.

Conclusions: The Cauchy 5 dome exhibits unusual radar polarization values consistent with a lack of embedded cm- to m-sized scatterers in the upper meter.

In contrast, Ina does not have low CPR values relative to the surrounding terrain. If any pyroclastics were produced at Ina, they likely formed a very fine layer and may have been intermixed with blocky regolith such that they are no longer visible to radar. Cataloging the presence and absence of pyroclastic deposits at the lunar hollows will help to determine whether the presence of volatiles was important to their formation.

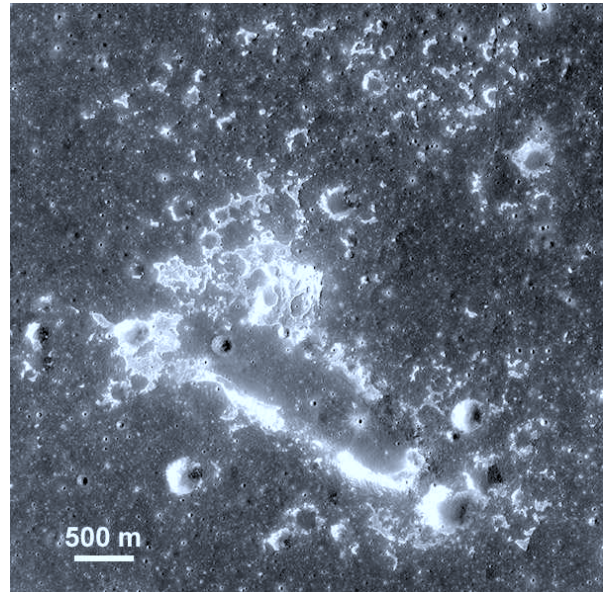


Fig. 2: High-resolution imaging of the Cauchy 5 dome reveals a linear caldera with surrounding hollow terrain. LROC NAC image M190351657.

Acknowledgements: This research was partially supported by a NASA Planetary Geology and Geophysics grant to L. Carter.

References: [1] Schultz, P. (1976) *Moon Morphology*, U. Texas Press. [2] El-Baz, F. (1973) *Apollo 17 Preliminary Science Report*, 30-13. [3] Schultz, P. et al. (2006) *Nature*, 444, 184. [4] Stooke, P. J. (2012) *LPSC 43*, Abstract #1011. [5] Garry, W. B. et al. (2012) *JGR*, 117, E00H31, doi:10.1029/2011JE003981. [6] Blewett, D. T. et al. (2011) *Science*, 333, 1856. [7] Garry, W. B. et al. (2008), *LPSC 39*, abstract 1734. [8] Raney, R. K. et al. (2011) *Proc. IEEE*, 99, 808. [9] Campbell, B. A. et al. (2010) *Icarus*, 208, doi:10.1016/j.icarus. 2010.03.011. [10] Hawke, B. R. and Coombs C. R., (1987) *LPSC 18*, 407. [11] Carter et al. (2009) *JGR*, 114, E11004, doi:10.1029/ 2009JE003406.